Biochemical Pharmacology 95 (2015) 1–15

Contents lists available at ScienceDirect

Biochemical Pharmacology

journal homepage: www.elsevier.com/locate/biochempharm

The native structure of annexin A2 peptides in hydrophilic environment determines their anti-angiogenic effects

Aase M. Raddum [a], Hanne Hollås [a], Igor A. Shumilin [b], Petra Henklein [c], Robert Kretsinger [b], Torgils Fossen [d], Anni Vedeler [a,*]

[a] Department of Biomedicine, University of Bergen
[b] University of Virginia, Charlottesville, USA
[c] Charité Universitätsmedizin, Berlin, Germany
[d] Centre for Pharmacy and Department of Chemistry, University of Bergen, Norway

ARTICLE INFO

Article history:
Received 9 January 2015
Accepted 27 February 2015
Available online 13 March 2015

Keywords:
Annexin A2
Peptide
Co-culture
Anti-angiogenenic
Folding

ABSTRACT

The progression of aggressive cancer occurs via angiogenesis and metastasis makes these processes important targets for the development of anti-cancer agents. However, recent studies have raised the concern that selective inhibition of angiogenesis results in a switch towards increased tumour growth and metastasis. Since Annexin A2 (AnxA2) is involved in both angiogenesis and metastasis, it may serve as an ideal target for the simultaneous inhibition of both processes. Based on the discovery that domains I (D_I) and IV (D_{IV}) of AnxA2 are potent inhibitors of angiogenesis, we designed seven peptides derived from these domains based on AnxA2 crystal structures. The peptides were expressed as fusion peptides to increase their folding and solubility. Light scattering, far-UV circular dichroism and thermal transition analyses were employed to investigate their aggregation tendencies, α-helical propensity and stability, respectively. 2,2,2-trifluoroethanol (50%) increased the α-helical propensities of all peptides, indicating that they may favour a hydrophobic environment, but did not enhance their thermal stability. D_I-P2 appears to be the most stable and folded peptide in a hydrophilic environment. The secondary structure of D_I-P2 was confirmed by nuclear magnetic resonance spectra. The effect of the seven AnxA2 peptides on the formation and integrity of capillary-like networks was studied in a co-culture system mimicking many of the angiogenesis-related processes. Notably, D_I-P2 inhibited significantly network formation in this system, indicating that the folded D_I-P2 peptide interferes with vascular endothelial growth factor-dependent pro-angiogenic processes. Thus, this peptide has the potential of being developed further as an anti-angiogenic drug.

1. Introduction

Angiogenesis is a tightly coordinated process involving the proliferation, directed migration and differentiation of cells. Additionally, cell–cell communication is highly essential, when new blood vessels form from an established vascular network [1,2]. A multitude of proteins, including growth factors and cytokines, regulate angiogenesis, with members of the vascular endothelial growth factor (VEGF) family acting as the main orchestrators [1,3,4]. During angiogenic growth, endothelial cells (ECs) present in the blood vessel wall are selected for sprouting by extracellular factors. The selected tip cells establish the growing sprout, while sprouting of neighbouring ECs is repressed. The surrounding ECs constituting the stalk of the new vessel sprout, actively divide to move the tip cells forward [1]. A prerequisite for migration is degradation of the extracellular matrix (ECM) in front of the tip cells. ECM breakdown is carried out by proteases, including plasminogen activators, which also indirectly enhance EC sprouting by releasing matrix-bound angiogenic activators, such as basic fibroblast growth factor, VEGF, transforming growth factor and by

Abbreviations: AnxA2, Annexin A2 protein; AnxA2-D_I, domain I of AnxA2; AnxA2-D_{IV}, domain IV of AnxA2; CD, circular dichroism; CSI, chemical shift index; ECM, extracellular matrix; ECs, endothelial cells; FL, full-length; GFP, green fluorescent protein; HUVECs, human umbilical vein endothelial cells; MBP, maltose binding protein; NMR, nuclear magnetic resonance; P, peptide; SMCs, pulmonary artery smooth muscle cells; TEV, tobacco etch virus; TFE, 2,2,2-trifluoroethanol; tPA, tissue plasminogen activator; VE-cadherin, vascular endothelial cadherin; VEGF, vascular endothelial growth factor; VEGFR, vascular endothelial growth factor receptor.

* Corresponding author at: Jonas Lies vei 91, N-5009 Bergen, Norway. Tel.: +47 55586435; fax: +47 55586360.
E-mail address: Anni.Vedeler@biomed.uib.no (A. Vedeler).

http://dx.doi.org/10.1016/j.bcp.2015.02.013

proteolytically activating angiogenic chemokines [5]. A tightly regulated balance of these factors in the ECM is crucial for the remodelling processes taking place during angiogenesis. Thus, insufficient ECM degradation will prevent vascular cells from leaving their original position, whereas excessive breakdown will remove critical support and guidance for migrating ECs and consequently inhibit angiogenesis [5]. In contrast to physiological angiogenesis, during tumour angiogenesis the balance of pro- and anti-angiogenic signals is completely deregulated, since the tumour itself secretes pro-angiogenic signals [5,6]. Tumour angiogenesis is critically important for the growth of solid tumours and is considered as one of the hallmarks of cancer [7,8]. It is recognised as an ideal therapeutic target, since most blood vessels are quiescent in adults [9], thus decreasing the probability of unwanted side-effects.

Annexin A2 (AnxA2) is a member of the ubiquitous Annexin protein family and is present in several intracellular compartments including the nucleus. However, it is also found extracellularly, associating with the ECM of certain cell types, such as ECs [10–13]. It is a multifunctional protein which binds to diverse intracellular ligands such as Ca^{2+}, S100A10 [10], membrane lipids [10–12], actin [14–16] and specific mRNAs [17,18]. Ligand binding, and thus the function of AnxA2, is regulated by its post-translational modifications. Extracellular AnxA2 acts as a co-receptor for tissue plasminogen activator (tPA) and plasminogen, resulting in increased local plasmin generation [19]. Interestingly, at cell–cell contact sites of confluent human umbilical vein endothelial cells (HUVECs), AnxA2 in complex with S100A10 is also found in conjunction with vascular endothelial (VE)-cadherin associating with cholesterol rafts. AnxA2 docks the VE-cadherin based complex to the actin cytoskeleton, providing mechanical strength to the adherens junctions [20]. Conversely, VEGF uncouples the AnxA2-S100A10 complex from the VE-cadherin based junction [20]. Moreover, phosphorylation of VE-cadherin is associated with weak junctions and impaired barrier function [21], which is increased in AnxA2-depleted ECs, emphasising a role for AnxA2 in the junction complex [22]. AnxA2 has been suggested to regulate endothelial morphogenesis via an adherens junction-mediated pathway upstream of Akt [22]. It also interacts with carcino-embryonic antigen cell adhesion molecule-1 (CEACAM1) [23], which is an extracellular transmembrane glycoprotein found at cell-cell contact sites of certain cell types, including activated ECs that participate in angiogenesis [24]. Furthermore, both proteins of the AnxA2-S100A10 complex [25,26] interact with the cell-cell adhesion molecule AHNAK [27], mediating its translocation from the cytosol to the inner surface of the plasma membrane, particularly in ECs forming specific blood-tissue barriers [28]. This indicates a complex role of AnxA2 in cell–cell adhesion. We have previously shown that domains I and IV of AnxA2 inhibit the formation of a vascular-like network in a co-culture system of HUVECs and smooth muscle cells (SMCs). In addition, these domains are able to disrupt a pre-formed network by interfering with VE-cadherin-mediated adhesion between the ECs [29].

Structurally, AnxA2 is a typical Annexin [30]. The unique 3 kDa N-terminal tail of AnxA2 consists of ~33 amino acid residues and folds into a structurally separate unit [31]. The convex surface of the tightly packed α-helical protein core structure contains the Annexin repeats, which are involved in the Ca^{2+}-dependent association of AnxA2 with membranes [10]. Both termini are present on the concave side of AnxA2 and are accessible for further interactions. The core structure of AnxA2 contains four domains, each composed of five α-helices (A-E) connected by short loops or turns [32]. Helices A and B as well as helices D-E are arranged in an approximately antiparallel manner in the full-length structure with helix C oriented almost perpendicular to the two pairs of helices [32]. We have been able to purify a soluble and partially folded form of AnxA2 domain IV by mutating hydrophobic amino acids involved in interfacial contacts with the other domains [33]. This domain as well as the soluble and fully folded domain I of AnxA2 showed potent anti-angiogenic effects when tested in the co-culture system [29].

Peptides are regarded as promising candidates in the development of novel drugs against a range of diseases. Several peptides are currently in therapeutic use, including peptide antibiotics such as the polymyxins and peptides derived from insulin and recombinant erythropoietin (EPO) for the treatment of diabetes, and anaemic and chronic renal failure patients, respectively [34]. The advantages of peptides over whole proteins or domains include high specificity and activity, fewer unspecific molecular targets, minimisation of drug–drug interactions and lack of immune responses in the host cell. Disadvantages include low bioavailability for oral administration, lower stability and immunogenic effects [35]. In the present study, seven peptides based on the amino acid sequence of domains I and IV of AnxA2 were designed, expressed as maltose binding protein (MBP)-fusion peptides and characterised for aggregation and secondary structure using light scattering assays and far-UV circular dichroism (CD) measurements, respectively, followed by functional testing for anti-angiogenic effects in the co-culture system.

2. Materials and methods

2.1. Protein purification

The expression and purification of the AnxA2 peptides as fusion peptides coupled to His-MBP were performed as described for AnxA2-D_I [29] and AnxA2-D_{IV} [33]. The primers used for the creation of the cDNAs encoding the peptides are listed in Table 1. Briefly, the fusion peptides were purified on His-Select Ni^{2+}-affinity resin (Sigma–Aldrich Co.; St. Louis, MO, USA), followed by elution of the His-tagged peptides and immediate loading on a PD-10 column (Sephadex G-25; GE Healthcare; Norway) equilibrated with the tobacco etch virus (TEV) cleavage/storage buffer (20 mM Tris, pH 8) (Sigma–Aldrich Co.; St. Louis, MO, USA). His-TEV protease cleaved peptides were separated from His-MBP, His-TEV and the uncleaved fusion peptides by a subsequent purification on His-Select Ni^{2+}-affinity resin (Sigma–Aldrich Co.; St. Louis, MO, USA), since the peptides do not bind to this resin.

2.2. Protein concentration determination

The concentration of His-MBP fusion peptides was determined using the Bradford method [36], while the concentration of the purified peptides was measured using the "Direct Detect" infrared spectroscopy quantitation system (Merck Millipore, Darmstadt, Germany), which takes advantage of the fact that proteins naturally vibrate due to stretching and bending of certain chemical groups along the polypeptide backbone and can absorb energy in the infrared region (www.millipore.com).

2.3. Light scattering assay

To study the aggregation tendencies of both the MBP-fusion peptides and the cleaved peptides, *in vitro* light scattering assays were performed [37]. Prior to light scattering assays, the His-MBP-fusion peptides in 20 mM Tris (pH 8) (Sigma–Aldrich Co.; St. Louis, MO, USA) were centrifuged for 30 min at 16000 × *g* at 4 °C to remove pre-formed aggregates. Assays (120 μl) were performed at 4 °C for 1 h with only the fusion peptide (1 mg/ml) in the cuvette, followed by addition of TEV protease (1:50 molar ratio) and further incubation for another 2 h. The aggregation rate of the fusion peptide/TEV-cleaved peptide was followed in real-time by light

Table 1

AnxA2 peptides	Direction	Sequence
DI-P1	Forward	5′-atccgggaagactc-**catgg**ggtcagtcaaagcgtacactaac-3′
	Reverse	5′-atccgggaagactg-**gtacc**tcagctgcggttggtcaggatgtt-3′
DI-P2	Forward	5′-atccgggaagactc-catgaagaaggaacttgcatcagcac-3′
	Reverse	5′-atccgggaagactg-**gtacc**ctatgttttcaataggcccaaaatcactg-3′
DIV-P1	Forward	5′-atccgggaagactt-**catgg**gtcagaacaagcccctgtattttgct-3′
	Reverse	5′-atccgggaagactg-**gtacc**tcagtccacttcactgcgcgagacc-3′
DIV-P2	Forward	5′-gtcac-**catgg**gcaagtccctgtactacta-3′
	Reverse	5′-atccgggaagactg-**gtacc**tcagtcatccccaccacacagg-3′
DIV-P3	Forward	5′-atccgggaagactt-catgggtagaacaagcccctgtcttatgctgacagactgtatgactcc-3′
	Reverse	5′-atccgggaagactg-**gtacc**tcagtccgattcactgcgcgagctc-3′
DIV-P4	Forward	5′-atccgggaagactc-**catgg**gcaagtccctgtactactatattcag-3′
	Reverse	5′-atccgggaagactg-**gtacc**tcagtcatccccaccacacagg-3′
DIV-P5	Forward	5′-atccgggaagactc-**catgg**aagtggacatgttgaaaat-3′
	Reverse	5′-atccgggaagactg-**gtacc**tcagtcatccccaccacacagg-3′

The underlined gaagac sequence refers to the *Bbs*I restriction enzyme recognition site to introduce *Nco*I and *Acc*65I compatible sites (indicated in bold) at the 5′ and 3′ ends, respectively. The *Bbs*I cleavage sites are indicated by hyphens. The DI-P2 and DIV-P3 have lost their *Nco*I sites due to codon usage to specify specific amino acids. All primers were supplied by Sigma.

scattering and measured by the increase in apparent absorption at 350 nm using an Agilent 8453 Diode Array Spectrophotometer with a Peltier temperature control unit.

2.4. Circular dichroism (CD)

Peptides (50–170 μM) were prepared in either 20 mM Tris (pH 8) or a 50% mixture of 2,2,2-trifluoroethanol (TFE) (Sigma–Aldrich Co.; St. Louis, MO) and 20 mM Tris (pH 8) to mimic behaviour in a hydrophobic environment. The far-UV CD spectra (185–260 nm, light path 1 mm) of the peptides were recorded at 20 °C in a Jasco J-810 spectropolarimeter equipped with a Peltier temperature control unit. The spectra obtained were the average of 4 scans. Buffer scans were subtracted from the peptide spectra. Due to the UV absorption of the Tris buffer components at short wavelengths the spectra shown in the Figures are cut at 195 nm to be in a reliable range. Thermal transition curves (10–70 °C) were determined by monitoring the decrease in ellipticity at 222 nm at a scanning rate of 40 °C/h using a 1 mm path length cuvette.

2.5. Purification and crystallisation of bovine AnxA2

Bovine full-length wt AnxA2 was expressed in the BL21 strain of *E. coli* as a recombinant MBP fusion protein from cDNA present in the pETM-41 vector (a kind gift from Gunter Stier, EMBL, Heidelberg) and cleaved from MBP during purification by TEV protease essentially as described [33]. The bovine AnxA2 crystals were grown at room temperature by the hanging drop method. The reservoir buffer contained 30% PEG 4000, 0.1 M Na acetate pH 4.6, 0.2 M ammonium acetate (Hampton Research, CA, USA). The drop consisted of 0.5 μl protein solution with the concentration of 2.3 mg/ml and 0.5 μl reservoir buffer supplemented with 20 μM $CaCl_2$ and 1 mM $MgCl_2$ (Sigma–Aldrich Co.; St. Louis, MO, USA). The bipyramidal crystals were formed within a week. The crystals belonged to the space group P212121 with unit cell parameters a = 48.3 Å, b = 63.3 Å and c = 117.3 Å and a single subunit of AnxA2 in the asymmetric unit.

X-ray diffraction data were collected from the crystal flash cooled with liquid N_2 and maintained at 100 K at the 19-BM beamline at Argonne National Laboratory. HKL-3000 [38] was used for the crystallographic data collection and processing, structure solution, and refinement. The structure of bovine AnxA2 was solved by molecular replacement using the structure of human AnxA2 (PDB: 1XJL) as a model. No electron density was observed for the N-terminal segment that included four extra residues resulting from the TEV cleavage site and first 21 residues of AnxA2. The structure was refined to R/R_{free} = 15.7%/20.9% at 2.0 Å resolution. Data collection and refinement statistics are presented

Table 2
Crystallographic analysis of bovine AnxA2.

Data collection	
Space group	P212121
Unit cell (Å/°)	a = 48.3, b = 63.3, c = 117.3, $\alpha = \beta = \gamma$ = 90.0
Resolution (Å)[a]	50.00–2.01 (2.08–2.01)
R_{merge}[a]	0.048 (0.276)
$I/\sigma(I)$[a]	37.6 (5.9)
No. of unique reflections	23260
Redundancy[a]	6.9 (6.4)
Completeness (%)[a]	99.7 (99.1)
Refinement	
R_{work}/R_{free} (%)	15.7/20.9
No. atoms	
Protein	2540
Ligand/Ion	4
Water	267
Mean B-factors (Å^2)	
Protein	38
Ligand/Ion	54
Water	45
R.m.s. deviations	
bond length (Å)	0.017
bond angle (°)	1.8
PDB code	4X9P

[a] Data for the highest resolution shell are shown in parentheses.

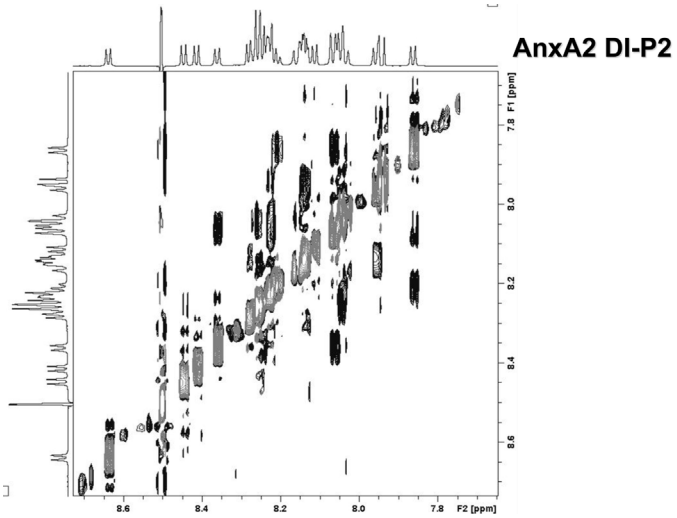

Fig. 1. 2D 1H TOCSY spectrum (grey) over layered with 2D 1H NOESY spectrum (black). Black signals without grey signals mainly indicate $NH/NH_{(i,i+1)}$ cross peaks and show that D_I-P2 contains secondary structure.

in Table 2. The coordinates and structure factors are deposited in the Protein Data Bank with accession code 4X9P.

2.6. Solid-phase peptide synthesis

The stepwise solid-phase synthesis of the peptide amide D_I-P2 was performed on an automated ABI 433A peptide synthesizer from Applied Biosystems on a 0.1 mM scale, using conventional Fmoc/tBu strategy (N,N,N′,N′-Tetramethyl-O-(1H-benzotriazol-1-yl)uronium hexafluorophosphate (HBTU), N,N-Diisopropylethylamine (DIEA), Nmethylpyrrolidone (NMP) (Sigma–Aldrich Co.; St. Louis, MO, USA)). As solid support preloaded H-Rink Amide-ChemMatrix resin (100 mg, loading 0.52 mmol/g) from PCAS BioMatrix Inc. was used. All amino acids were coupled according to standard methodologies in an automated single mode. Fmoc deprotection was carried out with 20% piperidine (Sigma–Aldrich Co.; St. Louis, MO, USA) in NMP. Cleavage of crude peptides from the resin was accomplished through treatment with 95% Trifluoroacetic acid (TFA) (Sigma–Aldrich Co.; St. Louis, MO, USA) 2.5% water, 2.5% Triisopropylsilane (TIPS) (Sigma–Aldrich Co.; St. Louis, MO, USA) for 1.5 h. Preparative purification by high-pressure liquid chromatography (HPLC) was carried out on a Shimadzu LC-8A system with a Sepserv ES (250 × 21.2 mm) column (Buffer A: 0.2% TFA in water, Buffer B: 0.2% TFA in water: acetonitrile, 1:4) (Sigma–Aldrich Co.; St. Louis, MO, USA). The purified peptides were dried by lyophilisation and characterised by analytical HPLC and mass spectral analysis [39].

2.7. NMR spectroscopy

Prior to NMR analysis of D_I-P2, the peptide was dissolved in 600 μl 50 mM aqueous phosphate buffer pH 7.0 containing 10% D_2O (v/v) (Sigma–Aldrich Co.; St. Louis, MO, USA) and transferred to a Wilmad 528-PP-7 NMR tube. TFE-D_2O was delivered by Cambridge Isotope Laboratories, Inc. (MA, USA). The 1D and 2D ^{1}H NMR experiments (Total Correlation Spectroscopy (TOCSY) and

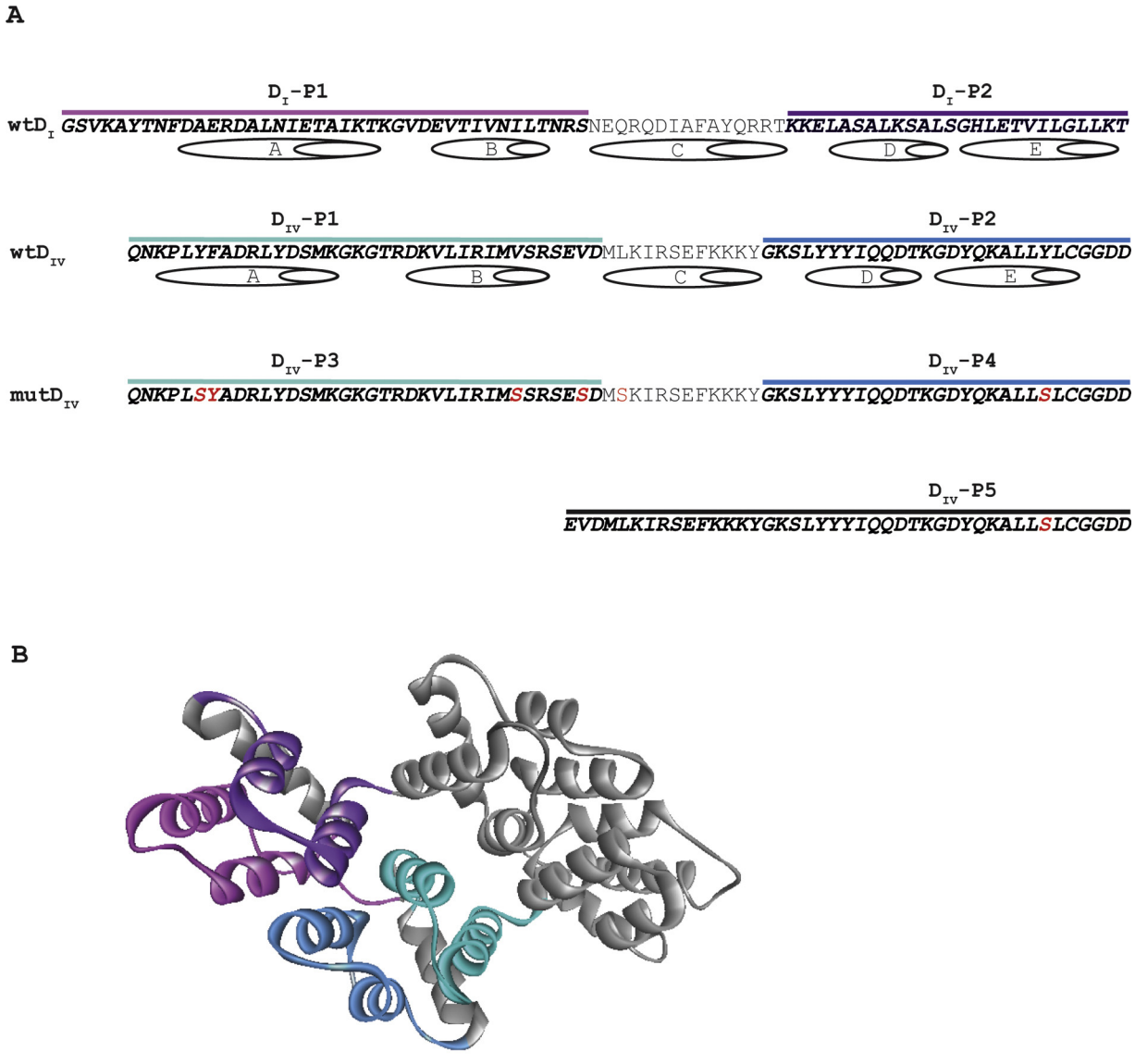

Fig. 2. Schematic presentation of the seven different AnxA2 peptides in the context of the bovine amino acid sequences of wt D_I, wt D_{IV} or mutated D_{IV} (A) and 3 dimensional structure of FL AnxA2 (B). (A): Two peptides derived from each of wt AnxA2 domains I (D_I-P1 and D_I-P2) and IV (D_{IV}-P1 and D_{IV}-P2) and three peptides derived from the mutated domain IV (D_{IV}-P3, D_{IV}-P4 and D_{IV}-P5) are indicated by solid lines above the linear amino acid sequences. The α-helices (A-E) are indicated by barrels below the amino acid sequences. The mutations introduced into AnxA2-D_{IV} to render it more soluble are indicated in red letters. (B): The structure of AnxA2 is based on the crystal structure of bovine AnxA2 (Protein data bank (PDB) code: 4X9P). The colour code of the respective peptide amino acid sequences in (A) is also used in (B). K88 in helix D and E96 in helix E in AnxA2-D_I are underlined.

Nuclear Overhauser Effect Spectroscopy (NOESY)) were performed at 600.13 MHz on a Bruker Avance 600 MHz instrument equipped with an UltraShield Plus magnet and a triple resonance cryoprobe with gradient unit [39]. The 2D NMR experiments were performed at 300 K without spinning with mixing times of 110 ms for the TOCSY experiments and 250 ms for the NOESY experiments, respectively (Fig. 1).

2.8. Co-culture assay

The co-culture assay has been described in detail earlier [40]. Briefly, green fluorescent protein (GFP)-expressing HUVECs and pulmonary artery SMCs were seeded simultaneously and cultured in EGM-2 cell medium (Lonza, Basel, Basel, Switzerland) for at least 72 h to ensure the formation of a stable network. The cells (5×10^4 SMCs and 10×10^3 HUVECs) were grown in a 96-well plate with 200 μl medium. When seeded simultaneously, an autonomous angiogenic programme is initiated that results in neovascular-like network formation. The peptides were added to the seeded co-cultures after 2 h. Following a 72 h treatment, networks were imaged by fluorescence microscopy.

2.9. Microscopy and image analysis

A BD Pathway 855 bioimaging system (BD Biosciences) was used for automated quantitative analysis of the co-cultures in the wells. Statistical analysis of the acquired images was carried out with BD Image Data Explorer software. Images were acquired as 2×2 montages using a 10x lens. In particular, the branching and tube network formation was followed by automated high-throughput imaging of live cells using the AttoVision v1.6.1 programme that makes a 1-pixel wide representation of the network by drawing a line through the middle of all the cellular "tubes" of the cellular network of the GFP-expressing ECs and the parameter "tube total length" was used throughout all the analyses. All data are representative of at least three independent experiments. The results are expressed as the mean (± SEM) from multiple (at least three) experiments. Statistical significance was determined using the two-tailed Student's *t*-test and *p*-values <0.05 were considered as significant.

3. Results

3.1. Design and purification of the peptides

Seven different peptides (P) of bovine AnxA2 were designed (Fig. 2A and B) and expressed as C-terminal fusion peptides, coupled to maltose binding protein (MBP) to increase their stability and solubility during expression and purification. As indicated in Fig. 2A, the peptides vary in length from 29 to 44 amino acids. The peptides P1 and P2 are based on the wt AnxA2-D_I (D_I-P1 and D_I-P2) or wt AnxA2-D_{IV} (D_{IV}-P1 and D_{IV}-P2) sequences harbouring helices A-B and D-E, respectively. The last three peptides, namely D_{IV}-P3, D_{IV}-P4 and D_{IV}-P5 are based on the mutated D_{IV}-sequence harbouring helices A-B, D-E and C-D-E, respectively. Consequently, D_{IV}-P1 and D_{IV}-P3 as well as D_{IV}-P2 and D_{IV}-P4 are corresponding peptides, only differing in one or a few amino acids. The mutations introduced into AnxA2-D_{IV} to render it more soluble are indicated in red letters (Fig. 2A) and include Y269S, F270Y, V293S and V298S in D_{IV}-P3 [33]. Peptides D_{IV}-P4 and D_{IV}-P5 harbour the Y333S mutation. With the exception of D_{IV}-P5, each peptide was designed to harbour two anti-parallel α-helices of the full-length (FL) protein to increase folding and stability when separated from its fusion partner (MBP). D_{IV}-P5 contains the same sequence as D_{IV}-P4, but is extended to include the putative plasminogen/plasmin binding site [19]. Thus, it is longer than the other peptides (Fig. 2). Two anti-parallel α-helices often stabilise each other mainly through salt bridge formation and hydrophobic interactions [42]. Close examination of the crystal structure of bovine AnxA2 (PDB ID: 4X9P) and lower resolution structures of human AnxA2 [32,43] shows that only peptide D_I-P2 appears to be stabilised by a salt bridge between Lys88 in helix D and Glu96 in helix E in the FL AnxA2 structure (Fig. 2A, underlined). However, this could not be confirmed by NMR (results not shown). Helices A and B present in D_I-P1, helix D in D_I-P2, helix A in D_{IV}-P1 and D_{IV}-P3, helices D and E in D_{IV}-P2 and D_{IV}-P4 as well as helices C, D and E in D_{IV}-P5 are partly exposed in the FL AnxA2 protein (Fig. 2B).

The His-MBP-fusion peptides could be purified in a soluble state, either as truly soluble molecules or present in soluble inclusion bodies due to their fusion with MBP [44] (Fig. 3A). However, in order to merit further investigation for a possible therapeutic use, it is crucial that the peptides themselves are soluble upon cleavage from the fusion partner. We were able to purify all seven AnxA2 peptides (Fig. 3B), however, it appears that D_{IV}-P3 has undergone partial proteolytic degradation, most likely in the host bacteria (Fig. 3B, lane 14). Apparently, D_{IV}-P2, D_{IV}-P4 and D_{IV}-P5 formed a minor proportion of dimers as indicated by analysis in 10–20% Tris-tricine gels (Fig. 3B, lanes 13, 15 and 16, respectively). It appeared that D_{IV}-P5 is more prone to cleavage with time (Fig. 3B, lane 16), most likely affecting the most N-terminal helix C, since this is not stabilised by interaction with another anti-parallel helix. Furthermore, it is possible that this extra cleavage site in D_{IV}-P5 is identical to the site cleaved by a plasmin-like protease between Lys307 and Arg308 (Lys308 in bovine AnxA2) [19], which is immediately preceding the D_{IV}-P4 region (Fig. 2A) producing a cleavage product (Fig. 3B, lane 16), with a size similar to that of D_{IV}-P4 (Fig. 3B, lane 15).

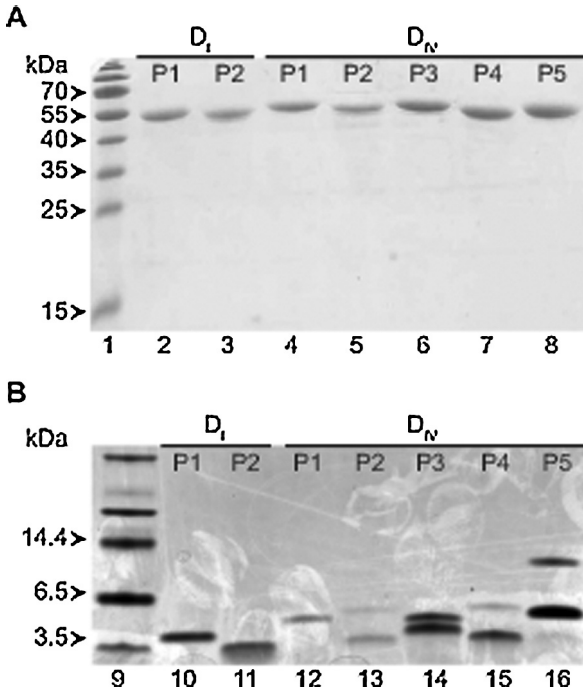

Fig. 3. Gel analysis of purified His-MBP-AnxA2 fusion peptides (A) and TEV-cleaved AnxA2 peptides (B). (A): ~10 μg of the Ni^{2+}-affinity purified His-MBP-AnxA2 peptides D_I-P1, D_I-P2, D_{IV}-P1, D_{IV}-P2, D_{IV}-P3, D_{IV}-P4 and D_{IV}-P5 (lanes 2-8, respectively, as indicated), were analysed by 15% SDS-PAGE. (B): ~10 μg of the purified TEV protease-digested AnxA2 peptides D_I-P1, D_I-P2, D_{IV}-P3, D_{IV}-P4 and D_{IV}-P5 (lanes 10, 11, 14, 15 and 16, respectively), and ~5 μg of D_{IV}-P1, D_{IV}-P2 (lanes 12 and 13, respectively), were analysed on a 10-20% (w/v) Tris-tricine peptide gel (BioRad, CA, USA). Proteins were visualised by Coomassie Brilliant Blue staining. Selected protein molecular mass standards (lanes 1, 9 and 17) are indicated.

3.2. Aggregation tendencies of the AnxA2 peptides

The aggregation tendencies of the AnxA2 peptides were measured by light scattering assays 1 h before and 2 h after the cleavage of the MBP fusion partner by the TEV protease (Fig. 4). The assays were performed at 4 °C. Furthermore, when performed for D_I-P2 at 37 °C, similar results were obtained (results not shown). An increase in the absorbance at 350 nm is a quantitative measurement of protein aggregation with no contribution from the absorbance of aromatic amino acids [45]. Also, it should be noted that the addition of the TEV protease results in an apparent increase in absorbance at approximately 60 min (Fig. 4), due to the opening of the lid of the instrument. The light scattering measurements of the TEV protease alone indicated no aggregation tendency (results not shown).

D_I-P2, D_{IV}-P2, D_{IV}-P4 and D_{IV}-P5 demonstrate a slight initial tendency to aggregate when fused to MBP (Fig. 4B, D, F and G, 0-20 min), whereas none of the cleaved peptides appear to aggregate at the concentrations used in the assays (1 mg/ml) (Fig. 4). In order to determine the efficiency of TEV cleavage of the peptides, samples taken directly from the cuvette at the end of the light scattering assays (after 3 h) were subjected to SDS-PAGE and Coomassie Brilliant Blue staining. The cleavage of the fusion peptides by the TEV protease was partial (Fig. 4H) during the time of measurement, but resulted in sufficient free peptides to enable the measurement of their aggregation tendencies. The uncleaved fusion peptides (46–51 kDa), as well as cleaved MBP (43 kDa) are visible by SDS-PAGE (Fig. 4H) while the peptides are too small to be seen on a 10% SDS-PAGE. In conclusion, none of the cleaved AnxA2

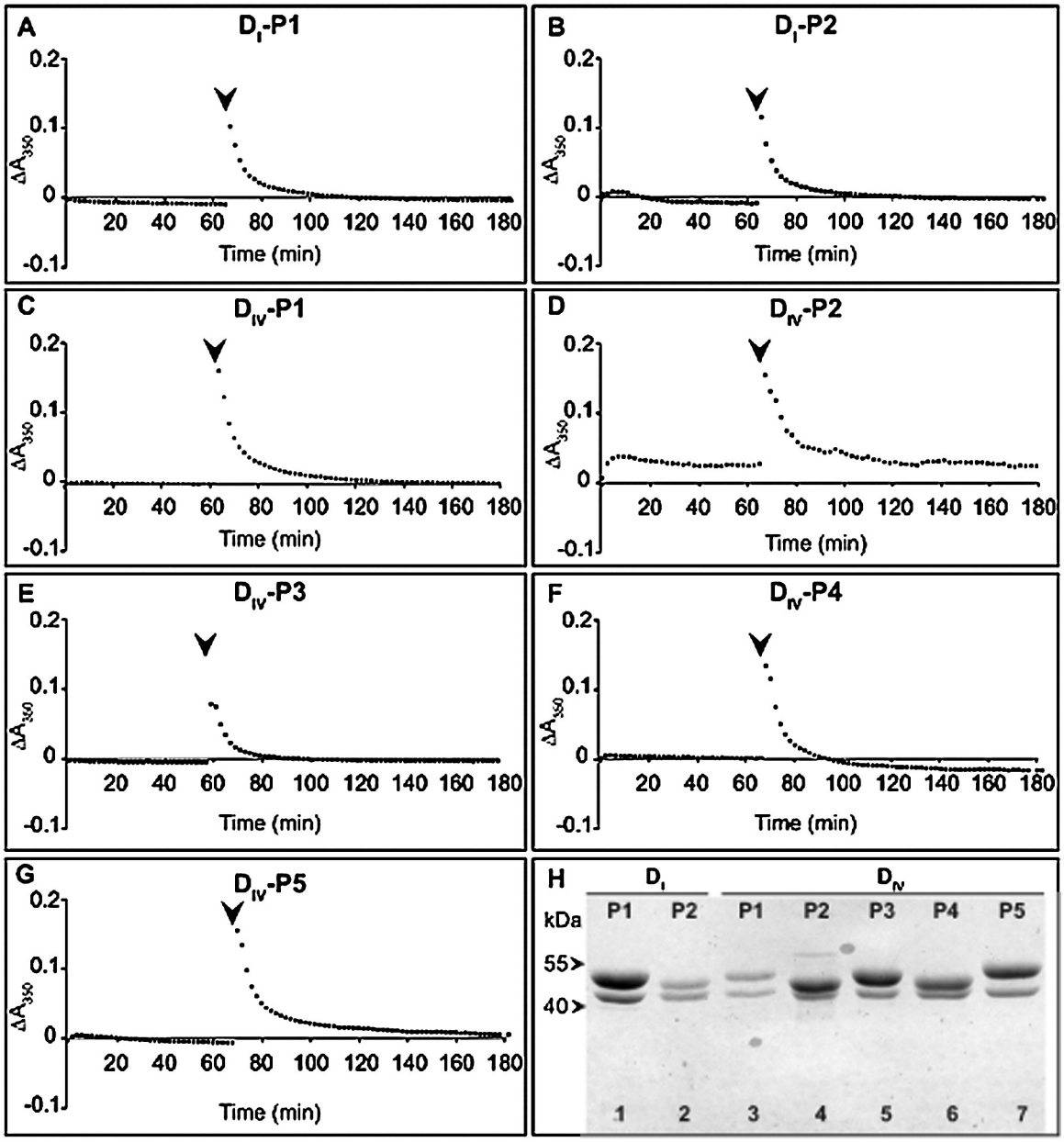

Fig. 4. Aggregation tendencies of the AnxA2 peptides before and after cleavage from His-MBP, followed in real-time by light scattering. The changes in light scattering of the AnxA2 peptides (1 mg/ml) measured at 350 nm (4 °C) are expressed as ΔA_{350} by subtracting background (20 mM Tris buffer; pH 8). The time of addition of TEV (1:50 molar ratio) is indicated by arrowheads. The aggregation tendencies of D_I-P1, D_I-P2, D_{IV}-P1, D_{IV}-P2, D_{IV}-P3, D_{IV}-P4 and D_{IV}-P5 are shown in A, B, C, D, E, F and G, respectively. Panel H indicates the degree of cleavage of the MBP fusion peptides after 2 h incubation with TEV at the end of the light scattering assays with D_I-P1, D_I-P2, D_{IV}-P1, D_{IV}-P2, D_{IV}-P3, D_{IV}-P4 and D_{IV}-P5 in lanes 1, 2, 3, 4, 5, 6 and 7, respectively. His-MBP-AnxA2 fusion peptides, His-MBP and peptides were separated by 10% SDS-PAGE and visualised by Coomassie Brilliant Blue staining.

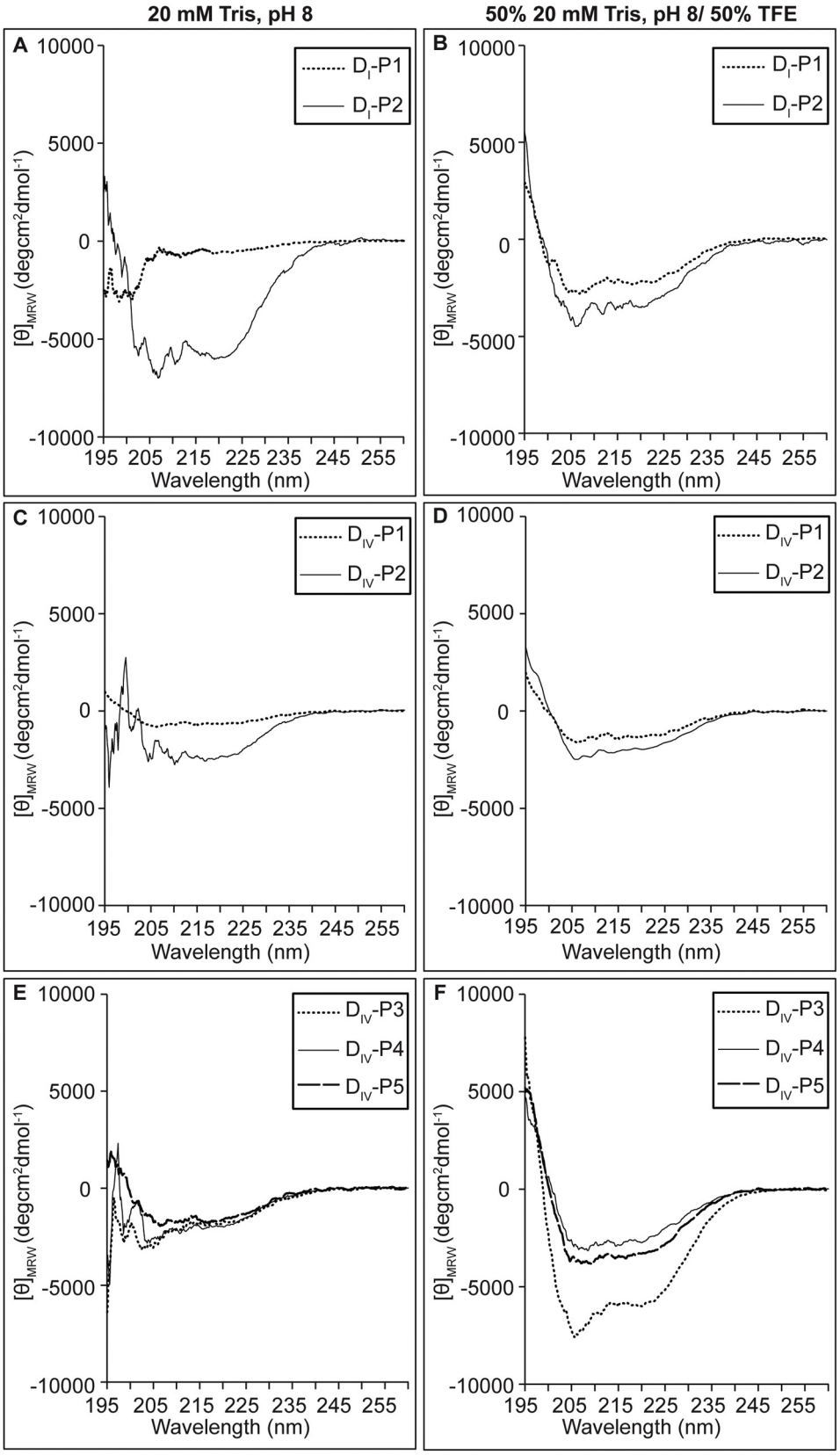

Fig. 5. Far-UV CD spectra of the AnxA2 peptides at 20 °C. The far-UV CD spectra were recorded for (A) (50-120 μM) D_I-P1 and D_I-P2 in Tris buffer (pH 8) or (B) 50% TFE/Tris buffer (pH 8). Similarly, the far-UV CD spectra were recorded for (70–170 μM) (C+D) D_{IV}-P1 and D_{IV}-P2 and (E and F) D_{IV}-P3 - D_{IV}-P5 in (C+E) Tris buffer (pH 8) or (D+F) 50% TFE/Tris buffer (pH 8), respectively, as indicated. Spectra were background corrected and the observed optical activity is expressed as the mean residue molar ellipticity [θ]MRW (deg cm^2 dmol^{-1}).

peptides appear to aggregate under the conditions and during the duration of the light scattering assays (Fig. 4).

3.3. Secondary structure and stability of the AnxA2 peptides

The AnxA2 peptides were subjected to far-UV CD analysis to elucidate their secondary structures both in an aqueous buffer (20 mM Tris of pH 8) (Fig. 5A, C and E) and in 50% TFE/Tris buffer of pH 8 (Fig. 5B, D and F). D_{IV}-P1, D_{IV}-P2, D_{IV}-P3 and D_{IV}-P4 appear to be relatively unstructured in 20 mM Tris (pH 8) buffer (Fig. 5C and E), but with a certain degree of α-helical content. By contrast, D_I-P2, and D_{IV}-P5, display a structural conformation in aqueous solution (Fig. 5A and E) with spectra that are characteristic of a predominantly α-helical structure with a double minima at 222 and 208 nm and a maximum band around 190-195 nm. By far, D_I-P2 appears to be the most folded peptide of these two peptides. The strong negative band at 198 nm suggests that D_I-P1 (Fig. 5A) exists mainly as a random coil structure in Tris buffer (pH 8).

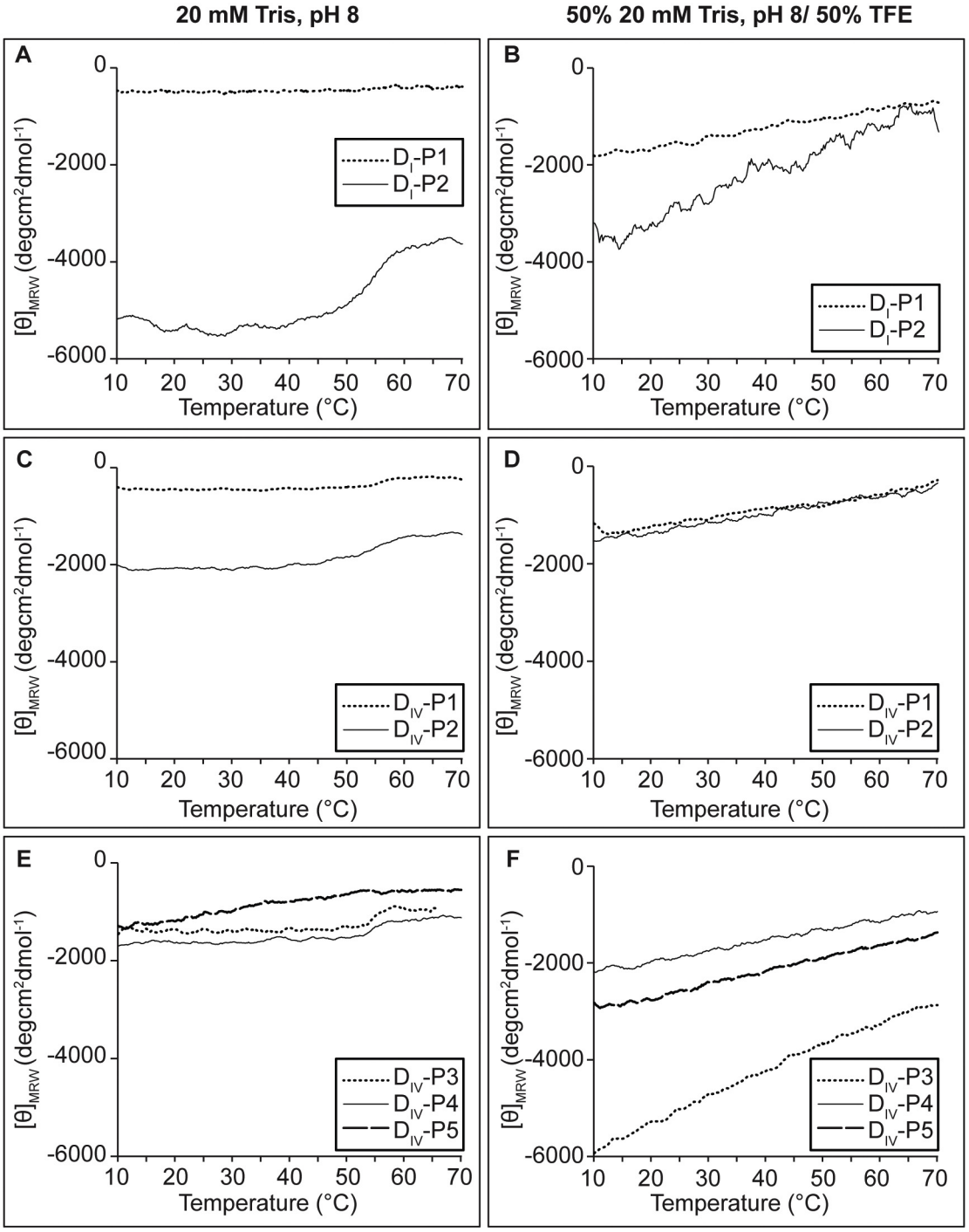

Fig. 6. CD-monitored thermal disruption of α-helicity of the AnxA2 peptides (range 10–70 °C). The change in ellipticity at 222 nm was measured at a heating rate of 40 °C/h in (A, C and E) Tris buffer (pH 8) or (B, D and F) 50% TFE/Tris buffer. The thermal transitions were recorded for (50-120 μM) (A) D_I-P1 and D_I-P2 in Tris buffer (pH 8) or (B) 50% TFE/Tris buffer (pH 8). Similarly, the far-UV CD spectra were recorded for (70-170 μM) (C) D_{IV}-P1 and D_{IV}-P2 and (D) D_{IV}-P3 - D_{IV}-P5 in Tris buffer (pH 8) or (E and F) 50% TFE/Tris buffer (pH 8), respectively. The observed optical activity is expressed as the mean residue molar ellipticity [θ]MRW (deg cm^2 $dmol^{-1}$). The apparent transition temperatures (T_m) were determined from the first derivative of the curve.

To investigate the relative stability of the AnxA2 peptides, thermal unfolding transitions (10-70 °C) were analysed by monitoring the molar ellipticity at 222 nm in Tris buffer, pH 8 (Fig. 6A,C and E) and 50% TFE/Tris buffer (Fig. 6B, D and F). AnxA2-D_I-P2, but not D_I-P1, exhibits a co-operative unfolding temperature transition in Tris buffer, pH 8 (Fig. 6A) with a midpoint melting temperature T_m of 54 ± 1 °C, while in 50% TFE neither of the two AnxA2-D_I peptides show this behaviour (Fig. 6B) as the thermal transition measurements indicate no clear melting temperatures. Thus, the α-helical structure of the two AnxA2-D_I peptides appeared to be unstable in 50% TFE at higher temperatures (Fig. 6B).

All the AnxA2 peptides derived from domain IV exhibit a certain degree of co-operative thermal unfolding transition in Tris buffer, pH 8, except D_{IV}-P5 (Fig. 6C and E). In each case, the co-operative transitions have T_m's of 55 ± 2 °C. The initial linear part of the thermal transition of these peptides (except D_{IV}-P5) may correspond to changes in their helicity that occur before the onset of the cooperative unfolding. Except for D_{IV}-P5, all AnxA2 peptides appear to be stable in aqueous buffer until about 50 °C, as indicated by the initial linear part of the CD thermal transition curves. They did not exhibit this behaviour in 50% TFE solvent (Fig. 6B, D and F), suggesting that the induced α-helical conformation of most of the AnxA2 peptides in 50% TFE solvent is not reflected in the stability of their secondary structure in the same solvent.

3.4. Secondary structure of AnxA2-D_I-P2 peptide

To obtain further structural information about the most folded of the AnxA2 peptides, D_I-P2, NMR spectra were obtained of the peptide in H_2O-D_2O (9:1) and H_2O-TFE (1:1). It has been shown experimentally that α-proton chemical shifts greater than 0.1 ppm relative to the random coil values are qualitative indicators of protein secondary structure. A minimum of four adjacent residues with an upfield shift are indicative of an α-helix, whereas β-sheets require a minimum of three residues with downfield shifts [46]. After spectral assignment, chemical shift index (CSI) plots were made (Fig. 7) to indicate the location of the α-helical structure. The peptide is structured (α-helical) both in aqueous solution and in a more hydrophobic environment (H_2O-TFE). The localisation of structure appears to be the same in both cases (Fig. 7), which is in agreement with the corresponding CD spectra of D_I-P2 (Fig. 5). The CD spectra of peptide D_I-P2 indicate relatively similar proportions of α-helical structure of the peptide both in aqueous and H_2O-TFE solution (Fig. 5). However, the CSI plots showed that the α-helical structure is best defined when the peptide is present in hydrophobic environment (Fig. 7; Tables 2 and 3). This may be accounted for by the fact that CD spectroscopy is rather indicative with respect to determination of exact proportions of α-helical structure when compared with NMR spectroscopy, which provides structural information at atomic resolution. The positive chemical shift deviation of Hα of G15 could indicate that this residue acts as a helix breaker. However, the crosspeaks at δ 4.27/8.50 (Hα S14/HN L17), δ 4.00/8.50 (Hα G15/HN L17) δ 8.34/8.23 (HN S14/HN G15), δ 8.83/8.23 (HN L13/HN G15), δ 8.34/8.21 (HN S14/HN H16) and δ 8.23/8.50 (HN G15/HN L17) observed in the NMR spectra of D_I-P2 recorded in TFE-H_2O, typical for peptides with α-helical structure, support the presence of a continuous α-helix, in which G15 is incorporated (Tables 3A and B).

3.5. D_I-P2 potently inhibits the formation of a vascular-like network in the co-culture system

To identify the regions of domains I and IV of AnxA2 containing the important secondary structure (or site) that mediate their anti-angiogenic effect, AnxA2 peptides (15 μM) were analysed for their potential inhibitory effects on capillary-like network formation in the co-culture system (Fig. 8). Notably, only D_I-P2 inhibited strongly the formation of a network (Fig. 8D), diminishing the tube total length value by approximately 60 ± 10% (Fig. 8J). Furthermore, in its presence the cells became more rounded in shape as compared to the elongated control cells (Fig. 8A). Similar inhibition on network formation and effect on cell morphology were observed in the presence of PTK787, an inhibitor of the VEGF receptor-2 (VEGFR-2) [47] (Fig. 8B and J). The other AnxA2 peptides inhibit network formation only slightly at this concentration, except for D_{IV}-P5, which inhibits the process by approximately 20-30% (Fig. 8I and J). Investigation of the dose-response effect of D_I-P2, the most potent anti-angiogenic peptide, showed that increasing the peptide concentration from 7.5 μM to 30 μM increased the inhibition of network formation from 20% to 60% (±10%) (Fig. 9E), indicating a clear dose–response relationship. However, none of the AnxA2 peptides were able to disintegrate an already formed capillary-like network (Fig. 10).

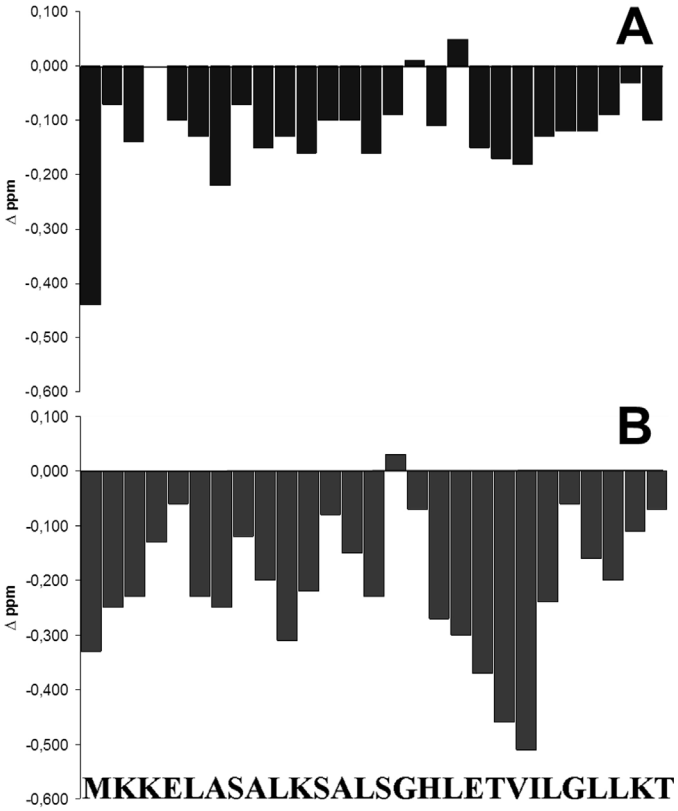

Fig. 7. CSI plot. Chemical shift differences (ppm) of the α-protons between the experimental values and those for residues in a random coil for the peptide AnxA2 D_I-P2 in (A) aqueous solution (H_2O-D_2O 9:1; v/v) at pH 3 and in (B) 50% aqueous TFE-D_2O at pH 3 at 300 K.

4. Discussion

4.1. Purification and characterisation of the AnxA2 peptides

AnxA2 plays a key role in angiogenesis and is therefore an attractive target for cancer therapy [48]. Silencing of AnxA2 inhibits tumour growth, migration and thus invasion of hepatoma cells [49]. Since it is a multifunctional protein, knocking down its mRNA by siRNA or RNAi treatment may severely affect its other cellular functions. Furthermore, antibody-based therapy targeting extracellular AnxA2 may also have other major drawbacks in addition, such as high production costs and low efficiency of drug

Table 3A
1H chemical shifts of ANX-A2-DI-P2 in H2O-D2O (9:1; v/v) at 298 K.

	HN	Hα	Hβ	Hγ	Hδ	Hε	NH2	Ar H
M1		4.08	2.11	2.54		2.06		
K2	8.69	4.29	1.73	1.36	1.63	2.93	7.48	
K3	8.46	4.22	1.71	1.36	1.64	2.93	7.48	
E4	8.50	4.29	1.99/1.88	2.32				
L5	8.30	4.28						
A6	8.33	4.22	1.35					
S7	8.19	4.28	3.81					
A8	8.19	4.28	1.35					
L9	8.01	4.23	1.59	1.53	0.86/0.82			
K10	8.19	4.23	1.79	1.62	1.72	2.93	7.48	
S11	8.16	4.34	3.81					
A12	8.28	4.25	1.35					
L13	8.09	4.28	1.59	1.59	0.85			
S14	8.10	4.34	3.82					
G15	8.31	3.88						
H16	8.28	4.64	3.22/3.11					8.55/7.21
L17	8.29	4.27	1.58	1.51	0.86/0.81			
E18	8.41	4.34	2.04/1.93	2.37				
T19	8.11	4.20	4.09	1.13				
V20	8.09	4.01	1.98	0.85				
I21	8.21	4.05	1.79	1.42/1.11 0.82/0.77				
L22	8.31	4.25	1.63	1.58	0.87/0.82			
G23	8.26	3.85						
L24	7.91	4.26	1.55	1.55	0.83			
L25	8.11	4.29						
K26	8.28	4.33	1.81	1.63	1.72	2.94	7.48	
T27	7.99	4.25	4.18	1.14				

delivery due to competition with IgGs circulating in the blood [50]. Therefore, peptides are attractive as potential therapeutic agents and in fact have been used with success as anti-angiogenic drugs [51], although their usefulness as therapeutic agents is limited by their aggregation tendency, which may cause reduced stability, loss of efficacy, the onset of unwanted immunogenic effects and false positive results due to nonspecific inhibition of receptors. Therefore, the stability of a given peptide as well as its structure needs to be studied and elucidated before concluding regarding its efficacy as a putative drug. It has been possible to obtain two of the domains of AnxA2 in a soluble form: Domain I (including 9 amino acids of the N-terminal tail), which possesses autonomous folding capacity [52], and a mutant domain IV which is capable of partial folding after the hydrophobic amino acids involved in interfacial contacts with the other domains have been mutated to hydrophilic ones [33]. As the design of the AnxA2

Table 3B
1H chemical shifts of AnxA2-DI-P2 in TFE-H2O (1:1; v/v) at 300 K.

	HN	Hα	Hβ	Hγ	Hδ	Hε	NH2	Ar H
M1		4.19	2.28/2.21	2.72/2.62		2.13		
K2	8.49	4.11	2.08			3.07	7.62	
K3	8.83	4.13	1.92	1.52	1.76	3.00	7.62	
E4	9.40	4.16	2.40/2.10	2.60				
L5	7.54	4.32	1.86	1.71	1.00			
A6	8.09	4.12	1.53					
S7	8.12	4.25	4.07/4.02					
A8	7.94	4.23	1.62					
L9	8.50	4.18	1.87	1.69	0.91			
K10	8.30	4.05	2.03	1.66/1.50	1.75	3.00	7.62	
S11	8.21	4.28	4.17/4.05					
A12	8.35	4.27	1.62					
L13	8.83	4.23	1.71	1.52	0.94			
S14	8.34	4.27	4.13/4.06					
G15	8.23	4.00						
H16	8.21	4.56	3.48/3.43					8.55 7.25
L17	8.50	4.11	1.88	1.79	0.97			
E18	8.51	3.99	2.31/2.20	2.64/2.49				
T19	7.71	3.98	4.41	1.35				
V20	7.74	3.72	2.34	0.96				
I21	8.32	3.72	1.97	1.23/0.96/0.86				
L22	8.41	4.14	1.90	1.57	0.93			
G23	7.90	3.95/3.87						
L24	8.26	4.22	2.09/1.89	1.60	0.91			
L25	8.51	4.18	1.86	1.69	0.91			
K26	8.13	4.25	2.03	1.66/1.59	1.75	3.03	7.62	
T27	7.81	4.28	4.39	1.36			7.33/6.99	

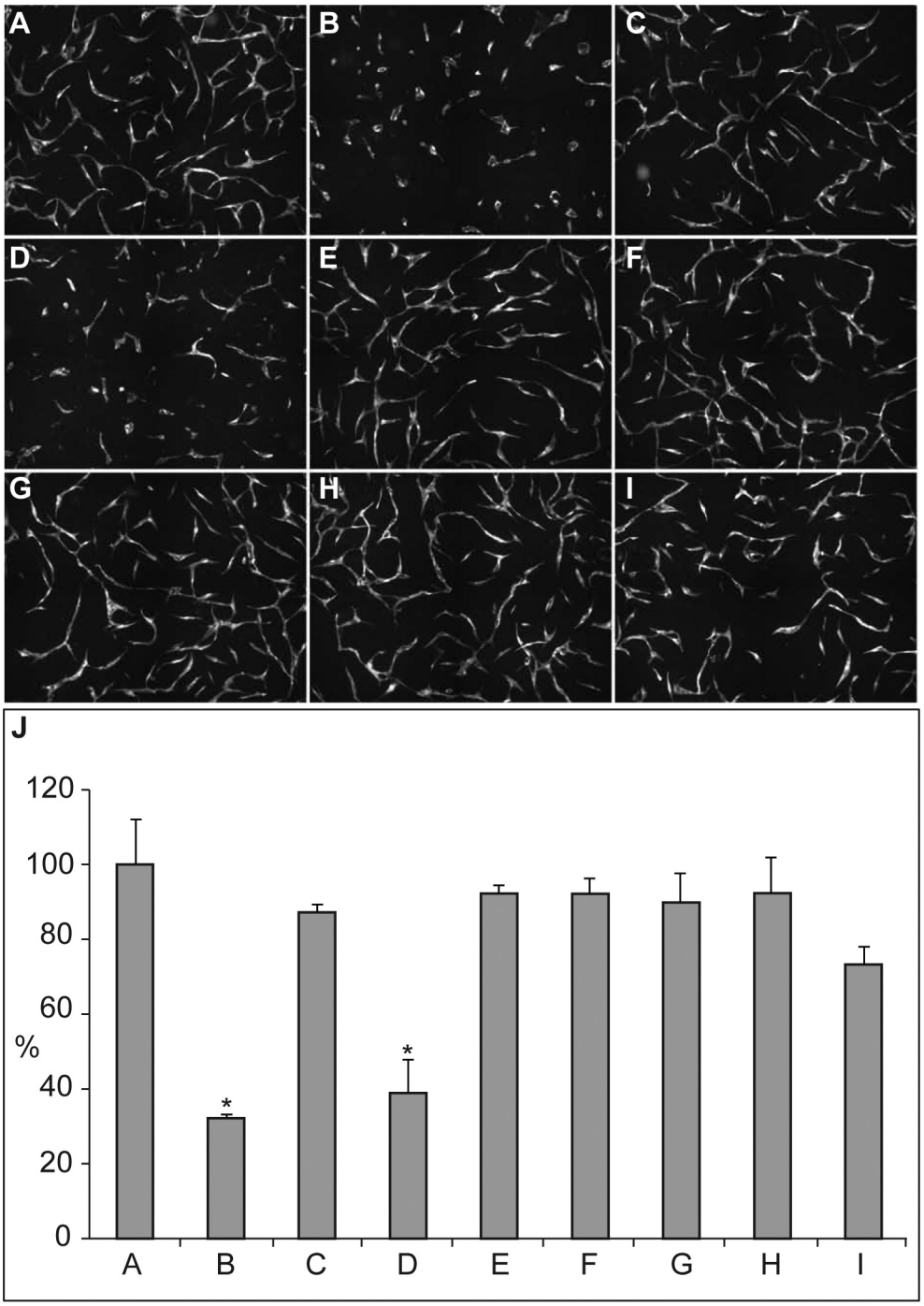

Fig. 8. Effect of the AnxA2 peptides on *in vitro* formation of a capillary-like network in co-cultures. Co-cultures of SMCs and GFP-expressing HUVECs were (A) untreated, or treated with (B) 100 nM PTK787, (C) 15 μM of D_I-P1, (D) D_I-P2, (E) D_{IV}-P1, (F) D_{IV}-P2, (G) D_{IV}-P3, (H) D_{IV}-P4, or (I) D_{IV}-P5 2 h after seeding. After 72 h incubation, images were taken at 10x magnification. The analysis of the tube total length (J) is expressed as percentage relative to the untreated control network (100%) (A), using the Attovision and BD Image Data Explorer programmes. Results (J) represent the mean ± SEM of 3 independent experiments. Statistical significance was determined by the two-tailed Student's t-test (*$P < 0.05$).

peptides was intended to promote higher stability and folding by containing regions that in the FL protein harbour two anti-parallel α-helices, it was of importance to determine if the design was successful in promoting α-helical secondary structure. Normally, the AnxA2 protein as well as its domains I and IV were stored in Tris buffer (pH 8), which is not ideal for CD measurements due to its high absorbance in the lower nm region. However, Tris buffer was preferred over phosphate buffer due to the inhibitory effect of the latter on network formation in the co-culture system (results not shown). Thus, due to UV absorption of the Tris buffer, accurate percentage calculations of secondary structure cannot be performed, while spectral comparisons are possible. It was also of interest to investigate whether the mutations initially introduced into the variant form of AnxA2-D_{IV} (see above) would stabilise an α-helical structure of the peptides in an aqueous environment (Fig. 5C and E, compare D_{IV}-P1 with D_{IV}-P3 and D_{IV}-P2 with D_{IV}-P4). Apparently, the mutations introduced in D_{IV}-P3 increased its α-helicity in the Tris buffer when compared to D_{IV}-P1 while the

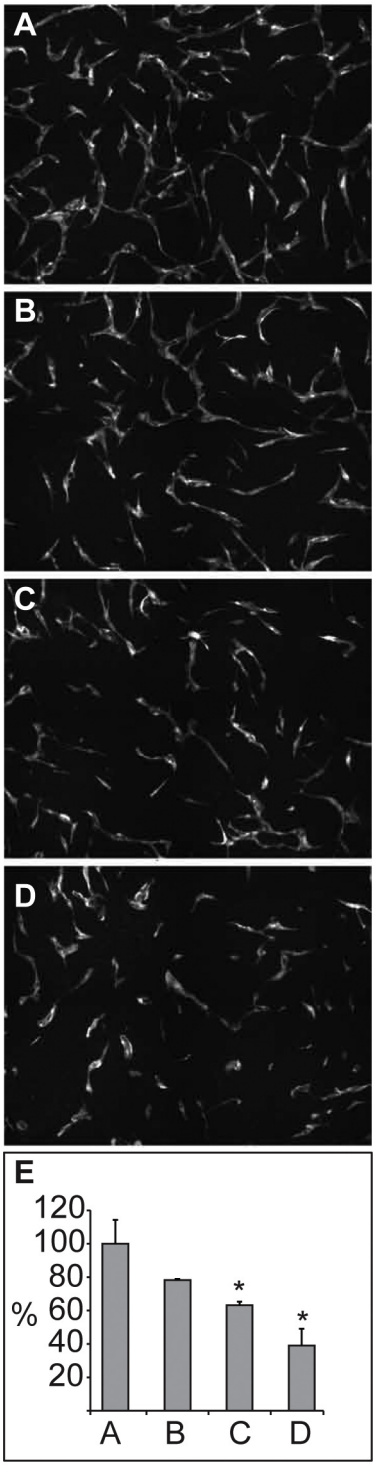

Fig. 9. The dose–response effect of D_I-P2 on *in vitro* formation of a capillary-like network. Co-cultures of SMCs and GFP-expressing HUVECs were (A) untreated, or treated with (B) 7.5 μM, (C) 15 μM, or (D) 30 μM D_I-P2 2 h after seeding. After 72 h incubation, images were taken at 10x magnification. The analysis of the tube total length (E) was performed as described in the legend to Fig. 8.

mutation in D_{IV}-P4 did not have the same effect when compared to D_{IV}-P2 (Fig. 5, compare C and E).

TFE stabilises α-helical structures via several mechanisms [53]. One possible mechanism is that TFE aggregates around the peptide forming a matrix that partly excludes water and thus mimics a hydrophobic environment. The matrix promotes the formation of local interactions and hence the formation of secondary structure [54]. In the presence of the α-helix inducing solvent, 50% TFE, all AnxA2 peptides gain various degrees of secondary α-helical structure, except D_I-P2 (Fig. 5, compare A, C and E with B, D and F). This implies that the AnxA2 peptides have a tendency to fold when present in a hydrophobic environment suggesting that they adopt a more folded conformation when associated with lipids in membranes.

The biophysical characterisations of the AnxA2 peptides indicate that D_I-P2 is the only α-helical peptide with a relatively high stability in aqueous solution. The pI values of the different AnxA2 peptides as determined by ExPASY [55] do not appear to affect their conformation since some are acidic (D_I-P1, D_{IV}-P2 and D_{IV}-P4 have pI values of 4.99, 4.78 and 4.78, respectively) while others are basic (D_I-P2, D_{IV}-P1, D_{IV}-P3 and D_{IV}-P2 have pI values of 9.40, 9.69, 9.69 and 9.30, respectively). The NMR data confirmed that peptide D_I-P2 is structured (α-helical) both in aqueous solution and in a more hydrophobic environment (H_2O-TFE). The localisation of structure appears to be the same in both cases (Fig. 7), although the CSI plots showed that the α-helical structure is best defined when the peptide is present in hydrophobic environment (Fig. 7).

4.2. D_I-P2 as a candidate for an anti-angiogenic therapeutic agent

Previously, we showed that domains I and IV of AnxA2 in low concentration (15 μM) strongly inhibit the formation of a capillary-like network in the co-culture system [29]. Activation of plasminogen did not appear to be important, while the disruption of the VE-cadherin-mediated contacts between ECs appeared to be an essential part of this effect [29]. In the present study, D_I-P2 was the only peptide that strongly inhibited the formation of a network of HUVECs grown on SMCs (Figs. 8 and 9). It should be noted that the inhibition of network formation appears to be less pronounced in Fig. 8J than in Fig. 9E, most likely due to the use of a slightly less dense population of HUVECs and/or lower degree of network formation (Fig. 9A). The inhibitory effects of the D_I-P2 peptide were consistent from experiment to experiment with the normal variation of displaying ±10%. Network formation in the co-culture system has been described in detail previously [40]. HUVECs transfected with either GFP or RFP are able to form a network on confluent SMCs, but not when cultured alone as monolayers, since network formation is dependent on SMC-derived VEGF [40]. The capillary-like network of HUVECs forms a lumen as evidenced by the luminal concentration of exogenously added TRITC-dextran, see Fig. 1 in [40]. The capillary-like tubules of ECs formed *in vitro* and the resulting vascular-like network possess many of the features observed *in vivo*, including deposition of basement membrane, formation of adherens junctions and lumen as well as the establishment of direct contacts between the two cell types [40]. Therefore, it is ideal as an initial imaging screening method. In contrast to domains I and IV of AnxA2 [29], none of the AnxA2 peptides were able to disrupt a pre-formed network in the co-culture system to a significant extent (Fig. 10). One possible explanation is that in the pre-formed vascular-like network, the mature, stable adherence junctions established between ECs, are not easily disrupted by small peptides. Alternatively, due to a putative lower affinity of the peptides compared to the domains, they may be inefficient in competing for binding with a ligand of endogenous AnxA2. One major difference between the formation of a network and the maintenance of a stable network in the co-culture system is the VEGF dependency. HUVECs in the co-culture system are totally dependent on SMC-derived VEGF to form a network, which cannot be replaced by exogenously added, soluble VEGF or other growth factors such as FGF. In contrast, when the network has been formed, the HUVECs become largely independent of this SMC-derived VEGF production [41]. Thus, it is possible that the peptide, D_I-P2, is able to

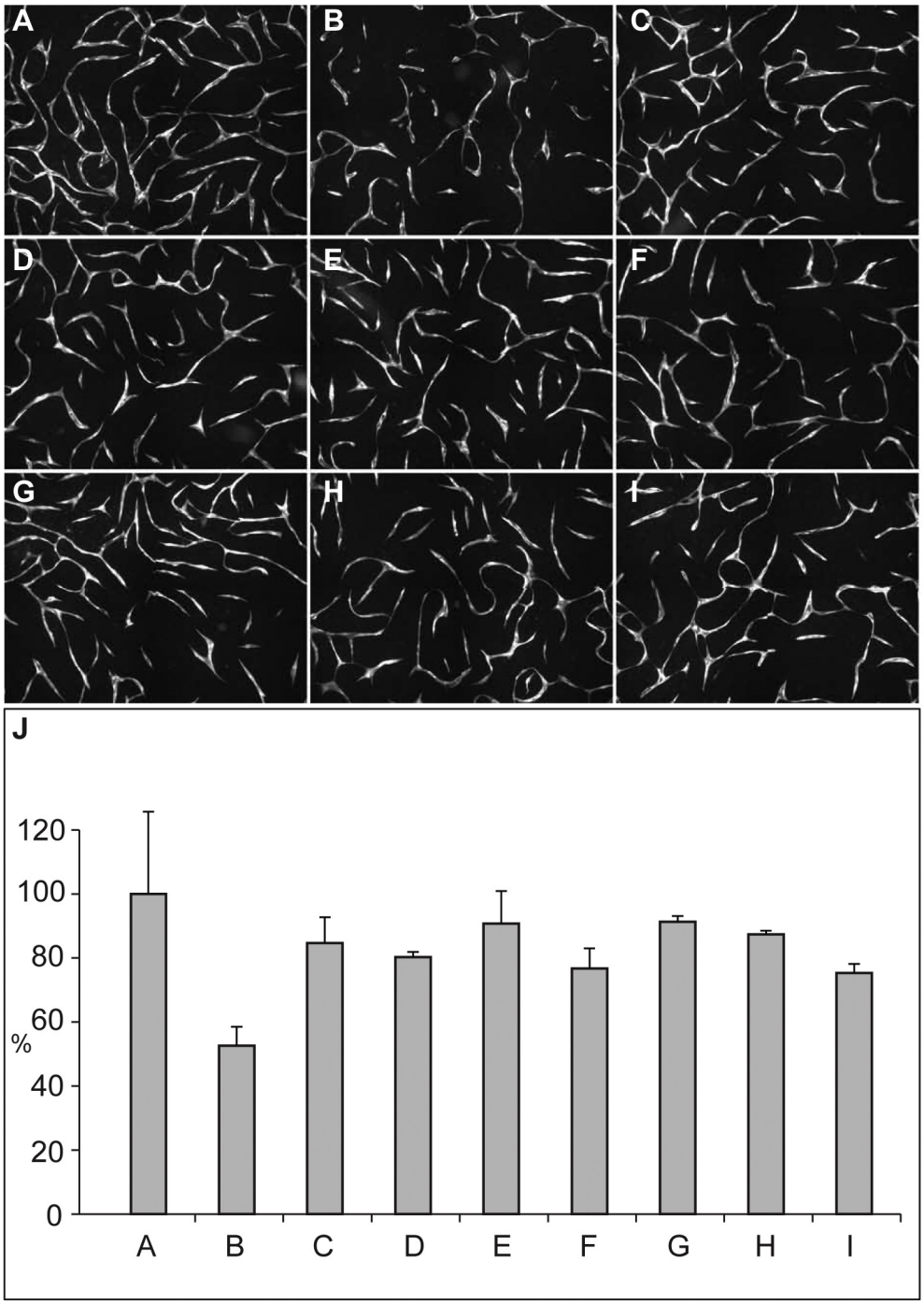

Fig. 10. The effect of the AnxA2 peptides on the integrity of pre-formed mature capillary-like networks. Co-cultures of SMCs and GFP-expressing HUVECs with a pre-formed network were (A) untreated, or treated with (B) 100 nM PTK787, 15 μM of (C) D_I-P1, (D) D_I-P2, (E) D_{IV}-P1, (F) D_{IV}-P2, (G) D_{IV}-P3, (H) D_{IV}-P4, or (I) D_{IV}-P5. After 72 h incubation, images were taken at 10x magnification. The analysis of the tube total length (E) was performed as described in the legend to Fig. 8.

interfere with the signaling via the VEGF-VEGFR2 pathway as reported for the FL AnxA2 protein during ischemia-induced retinal neoangiogenesis [56]. Therefore, it could be interesting to develop this peptide further for use in anti-angiogenic therapy.

AnxA2 may be involved in angiogenesis at several levels. It may (i) act as a co-receptor for tPA and plasminogen to generate plasmin [57], (ii) regulate the "locking" of VE-cadherin-based complex to lipid rafts and the actin cytoskeleton and/or (iii) modulate actin dynamics. A hexapeptide, LCKLSL, containing the tPA-binding site in the N-terminus of AnxA2, competes with endogenous AnxA2 and thus inhibits the generation of plasmin [58]. Another synthetic 36 amino acid long peptide derived from the venom of a scorpion (TM601) also inhibits the activation of plasmin by binding to AnxA2 [59]. However, our previous findings provide evidence that the anti-angiogenic effects of domains I and IV of AnxA2 are not due to their inhibitory effects on the activation of plasminogen [29].

In conclusion, a fast and relatively inexpensive strategy was adopted to express and purify AnxA2 peptides fused to MBP using bacteria. It is possible that MBP improves the solubility of the

peptides. Real time light scattering measurements were performed to provide estimates of the aggregation tendencies of the cleaved AnxA2 peptides. Based on the biophysical characterisations (far-UV CD and thermal transition measurements) of the AnxA2 peptides, it can be proposed that the inhibitory effect of D_I-P2 on the formation of a VEGF-dependent capillary-like network in the co-culture system (hydrophilic environment) is due to its α-helical conformational structure corresponding to those found in the FL native AnxA2 protein. The NMR data confirmed that the D_I-P2 peptide is structured (α-helical) in aqueous solution. Thus, the anti-angiogenic effect of D_I-P2 in the co-culture system does not appear to involve its unspecific binding to lipids, but rather its interference with AnxA2-mediated effects that are VEGF-dependent and based on its competition with endogenous extracellular AnxA2.

Acknowledgements

We are grateful to Gerd Nielsen, Asta Optun and Hanne Ravneberg for their excellent technical assistance. We also want to express our gratitude to Prof. Torgeir Flatmark and Dr. Lasse Evensen (University of Bergen, Norway) for valuable discussions. We are grateful to Prof. Jaakko Saraste (University of Bergen, Norway) for reading the manuscript and giving valuable comments. This study was funded by the University of Bergen and Helse Vest (grant no 911499), Norway.

References

[1] R.H. Adams, K. Alitalo, Molecular regulation of angiogenesis and lymphangiogenesis, Nat. Rev. Mol. Cell Biol. 8 (2007) 464–478.
[2] P. Saharinen, L. Eklund, K. Pulkki, P. Bono, K. Alitalo, VEGF and angiopoietin signaling in tumor angiogenesis and metastasis, Trends Mol. Med. 17 (2011) 347–362.
[3] P. Carmeliet, Angiogenesis in life, disease and medicine, Nature 438 (2005) 932–936.
[4] P. Carmeliet, VEGF as a key mediator of angiogenesis in cancer, Oncology 69 (2005) 4–10.
[5] P. Carmeliet, Angiogenesis in health and disease, Nat. Med. 9 (2003) 653–660.
[6] G. Bergers, L.E. Benjamin, Tumorigenesis and the angiogenic switch, Nat. Rev. Cancer 3 (2003) 401–410.
[7] D. Hanahan, R.A. Weinberg, The hallmarks of cancer, Cell 100 (2000) 57–70.
[8] D. Hanahan, R.A. Weinberg, Hallmarks of cancer: the next generation, Cell 144 (2011) 646–674.
[9] M. Potente, H. Gerhardt, P. Carmeliet, Basic and therapeutic aspects of angiogenesis, Cell 146 (2011) 873–887.
[10] V. Gerke, S.E. Moss, Annexins: from structure to function, Physiol. Rev. 82 (2002) 331–371.
[11] U. Rescher, V. Gerke, Annexins-unique membrane binding proteins with diverse functions, J. Cell Sci. 117 (2004) 2631–2639.
[12] V. Gerke, C.E. Creutz, S.E. Moss, Annexins: linking Ca^{2+} signalling to membrane dynamics, Nat. Rev. Mol. Cell Biol. 6 (2005) 449–461.
[13] P. Singh, Role of Annexin-II in GI cancers: interaction with gastrins/progastrins, Cancer Lett. 252 (2007) 19–35.
[14] N.R. Filipenko, D.M. Waisman, The C terminus of annexin II mediates binding to F-actin, J. Biol. Chem. 276 (2001) 5310–5315.
[15] M.J. Hayes, D. Shao, M. Bailly, S.E. Moss, Regulation of actin dynamics by annexin 2, EMBO J. 25 (2006) 1816–1826.
[16] A.G. Grieve, S.E. Moss, M.J. Hayes, Annexin A2 at the interface of actin and membrane dynamics: a focus on its roles in endocytosis and cell polarization, Int. J. Cell Biol. 2012 (2012) 852430.
[17] A. Vedeler, H. Hollas, Annexin II is associated with mRNAs which may constitute a distinct subpopulation, Biochem. J. 348 (2000) 565–572.
[18] A. Vedeler, H. Hollås, A.K. Grindheim, A.M. Raddum, Multiple roles of annexin A2 in post-transcriptional regulation of gene expression, Curr. Protein Pept. Sci. 13 (2012) 401–412.
[19] K.A. Hajjar, A.T. Jacovina, J. Chacko, An endothelial cell receptor for plasminogen/tissue plasminogen activator. I. Identity with annexin II, J. Biol. Chem. 269 (1994) 21191–21197.
[20] S. Heyraud, M. Jaquinod, C. Durmort, E. Dambroise, E. Concord, J.P. Schaal, P. Huber, D. Gulino-Debrac, Contribution of annexin 2 to the architecture of mature endothelial adherens junctions, Mol. Cell Biol. 28 (2008) 1657–1668.
[21] M.G. Lampugnani, M. Corada, P. Andriopoulou, S. Esser, W. Risau, E. Dejana, Cell confluence regulates tyrosine phosphorylation of adherens junction components in endothelial cells, J. Cell Sci. 110 (1997) 2065–2077.
[22] S.C. Su, S.A. Maxwell, Bayless KJ. Annexin 2 regulates endothelial morphogenesis by controlling AKT activation and junctional integrity, J. Biol. Chem. 285 (2010) 40624–40634.
[23] J. Kirshner, D. Schumann, J.E.C.E.A.C.A.M1 Shively, a cell-cell adhesion molecule, directly associates with annexin II in a three-dimensional model of mammary morphogenesis, J. Biol. Chem. 278 (2003) 50338–50345.
[24] S. Ergün, N. Kilik, G. Ziegeler, A. Hansen, P. Nollau, J. Götze, J.H. Wurmbach, A. Horst, J. Weil, M. Fernando, C. Wagener, CEA-related cell adhesion molecule 1: a potent angiogenic factor and a major effector of vascular endothelial growth factor, Mol. Cell 5 (2000) 311–320.
[25] B.R. Dempsey, A. Rezvanpour, T.W. Lee, K.R. Barber, M.S. Junop, G.S. Shaw, Structure of an asymmetric ternary protein complex provides insight for membrane interaction, Structure 20 (2012) 1737–1745.
[26] G. Ozorowski, C.M. Ryan, J.P. Whitelegge, H. Luecke, Withaferin A binds covalently to the N-terminal domain of annexin A2, Biol. Chem. 393 (2012) 1151–1163.
[27] C. Benaud, B.J. Gentil, N. Assard, M. Court, J. Garin, C. Delphin, J. Baudier, AHNAK interaction with the annexin 2/S100A10 complex regulates cell membrane cytoarchitecture, J. Cell Biol. 164 (2004) 133–144.
[28] B.J. Gentil, C. Benaud, C. Delphin, C. Remy, V. Berezowski, R. Cecchelli, O. Feraud, D. Vittet, J. Baudier, A.H.N.A.K. Specific, expression in brain endothelial cells with barrier properties, J. Cell Physiol. 203 (2005) 362–371.
[29] A.M. Raddum, L. Evensen, H. Hollås, A.K. Grindheim, J.B. Lorens, A. Vedeler, Domains I and IV of Annexin A2 affect the formation and integrity of in vitro capillary-like networks, PLoS One 8 (2013) e60281.
[30] R. Huber, J. Römisch, E.P. Paques, The crystal and molecular structure of human annexin V, an anticoagulant protein that binds to calcium and membranes, EMBO J. 9 (1990) 3867–3874.
[31] Y.H. Hong, H.S. Won, H.C. Ahn, B.J. Lee, Structural elucidation of the protein- and membrane-binding properties of the N-terminal tail domain of human annexin II, J. Biochem. 134 (2003) 427–432.
[32] A. Rosengarth, H. Luecke, A2. Annexin, Does it induce membrane aggregation by a new multimeric state of the protein, Annexins 1 (2004) 129–136.
[33] I. Aukrust, L. Evensen, H. Hollås, F. Berven, R.A. Atkinson, G. Travé, T. Flatmark, A. Vedeler, Engineering, biophysical characterisation and binding properties of a soluble mutant form of annexin A2 domain IV that adopts a partially folded conformation, J. Mol. Biol. 363 (2006) 469–481.
[34] C.M. Edwards, M.A. Cohen, S.R. Bloom, Peptides as drugs, QJM 92 (1999) 1–4.
[35] Y. Lu, J. Yang, E. Sega, Issues related to targeted delivery of proteins and peptides, AAPS J. 8 (2006) E466–E478.
[36] M.M. Bradford, A rapid and sensitive method for the quantitation of microgram quantities of protein utilizing the principle of protein-dye binding, Anal. Biochem. 72 (1976) 248–254.
[37] J. Leandro, N. Simonsen, J. Saraste, P. Leandro, T. Flatmark, Phenylketonuria as a protein misfolding disease: The mutation pG46S in phenylalanine hydroxylase promotes self-association and fibril formation, Biochim. Biophys. Acta 1812 (2011) 106–120.
[38] W. Minor, M. Cymborowski, Z. Otwinowski, M. Chruszcz, HKL-3000: the integration of data reduction and structure solution–from diffraction images to an initial model in minutes, Acta Crystallogr. D Biol. Crystallogr. 62 (2006) 859–866.
[39] Solbak SMØ, T.R. Reksten, F. Hahn, V. Wray, P. Henklein, P. Henklein, Ø. Halskau, U. Schubert, T. Fossen, HIV-1 p6 - a structured to flexible multifunctional membrane-interacting protein, Biochim. Biophys. Acta 1828 (2013) 816–823.
[40] L. Evensen, D.R. Micklem, W. Link, J.B. Lorens, Mural cell associated VEGF is required for organotypic vessel formation, PLoS One 4 (2009) e5798.
[41] L. Evensen, D.R. Micklem, W. Link, J.B. Lorens, A novel imaging-based high-throughput screening approach to anti-angiogenic drug discovery, Cytometry A 77 (2010) 41–51.
[42] L.K. Henchey, A.L. Jochim, P.S. Arora, Contemporary strategies for the stabilization of peptides in the alpha-helical conformation, Curr. Opin. Chem. Biol. 12 (2008) 692–697.
[43] C. Shao, F. Zhang, M.M. Kemp, R.J. Linhardt, D.M. Waisman, J.F. Head, B.A. Seaton, Crystallographic analysis of calcium-dependent heparin binding to annexin A2, J. Biol. Chem. 281 (2006) 31689–31695.
[44] Y. Nominé, T. Ristriani, C. Laurent, J.F. Lefèvre, E. Weiss, G. Travé, Formation of soluble inclusion bodies by hpv e6 oncoprotein fused to maltose-binding protein, Protein Expr. Purif. 23 (2001) 22–32.
[45] M.E. Cromwell, E. Hilario, F. Jacobson, Protein aggregation and bioprocessing, AAPS J. 8 (2006) E572–E579.
[46] D.S. Wishart, B.D. Sykes, F.M. Richards, The chemical shift index: a fast and simple method for the assignment of protein secondary structure through NMR spectroscopy, Biochemistry 31 (1992) 1647–1651.
[47] J. Drevs, R. Müller-Driver, C. Wittig, S. Fuxius, N. Esser, H. Hugenschmidt, M.A. Konerding, P.R. Allegrini, J. Wood, J. Hennig, C. Unger, Marmé D. PTK787/ZK 222584, a specific vascular endothelial growth factor-receptor tyrosine kinase inhibitor, affects the anatomy of the tumor vascular bed and the functional vascular properties as detected by dynamic enhanced magnetic resonance imaging, Cancer Res. 62 (2002) 4015–4022.
[48] M.C. Sharma, M. Sharma, The role of annexin II in angiogenesis and tumor progression: a potential therapeutic target, Curr. Pharm. 13 (2007) 3568–3575.
[49] H.J. Zhang, D.F. Yao, M. Yao, H. Huang, L. Wang, M.J. Yan, X.D. Yan, X. Gu, W. Wu, S.L. Lu, Annexin A2 silencing inhibits invasion, migration, and tumorigenic potential of hepatoma cells, World J. Gastroenterol. 19 (2013) 3792–3801.
[50] P. Chames, M. Van Regenmortel, E. Weiss, D. Baty, Therapeutic antibodies: successes, limitations and hopes for the future, Br. J. Pharmacol. 157 (2009) 220–233.
[51] K.C. Foy, M.J. Miller, N. Moldovan, Carson Iii WE, Kaumaya PT. Combined vaccination with HER-2 peptide followed by therapy with VEGF peptide mimics exerts effective anti-tumor and anti-angiogenic effects in vitro and in vivo, OncoImmunology 1 (2012) 1–13.

[52] F. Cordier-Ochsenbein, R. Guerois, F. Baleux, T. Huynh-Dinh, A. Chaffotte, J.M. Neumann, A. Sanson, Folding properties of an annexin I domain: a 1H-15 N NMR and CD study, Biochemistry 35 (1996) 10347–10357.
[53] P. Luo, R.L. Baldwin, Mechanism of helix induction by trifluoroethanol: a framework for extrapolating the helix-forming properties of peptides from trifluoroethanol/water mixtures back to water, Biochemistry 36 (1997) 8413–8421.
[54] D. Roccatano, G. Colombo, M. Fioroni, A.E. Mark, Mechanism by which 2,2,2-trifluoroethanol/water mixtures stabilize secondary-structure formation in peptides: a molecular dynamics study, Proc. Natl. Acad. Sci. USA 99 (2002) 12179–12184.
[55] E. Gasteiger, C. Hoogland, A. Gattiker, S. Duvaud, M.R. Wilkins, R.D. Appel, A. Bairoch, Protein identification and analysis tools on the ExPASy server, in: J.M. Walker (Ed.), The Proteomics Protocols Handbook, Humana Press, 2005, pp. 571–607.
[56] S. Zhao, L. Huang, J. Wu, Y. Zhang, D. Pan, X. Liu, Vascular endothelial growth factor upregulates expression of annexin A2 in vitro and in a mouse model of ischemic retinopathy, Mol. Vis. 15 (2009) 1231–1242.
[57] Q. Ling, A.T. Jacovina, A. Deora, M. Febbraio, R. Simantov, R.L. Silverstein, B. Hempstead, W.H. Mark, K.A. Hajjar, Annexin II regulates fibrin homeostasis and neoangiogenesis in vivo, J. Clin. Invest. 113 (2004) 38–48.
[58] M. Valapala, S.I. Thamake, J.K. Vishwanatha, A competitive hexapeptide inhibitor of annexin A2 prevents hypoxia-induced angiogenic events, J. Cell Sci. 124 (2011) 1453–1464.
[59] K. Kesavan, J. Ratliff, E.W. Johnson, W. Dahlberg, J.M. Asara, P. Misra, J.V. Frangioni, D.B. Jacoby, Annexin A2 is a molecular target for TM601, a peptide with tumor-targeting and anti-angiogenic effects, J. Biol. Chem. 285 (2010) 4366–4374.